IJEAST

INTERNATIONAL JOURNAL
OF ENGINEERING APPLIED SCIENCE
AND TECHNOLOGY

VOLUME : 9 ISSUE : 10 Print / Issue Publication Date: 21-Apr-2025

ISSN : 2455-2143

DOI : 10.33564/IJEAST.2025.v09i10.005

Indexed In

Google SCHOLAR OPEN ACCESS doi Crossref

WWW.IJEAST.COM

editor@ijeast.com

International Journal of Engineering Applied Sciences and Technology, 2025
Vol. 9, Issue 10, ISSN No. 2455-2143, Pages 50-72
Published Online February 2025 in IJEAST (http://www.ijeast.com)

ANALYSIS OF EEMD BASED RESIDUAL SIGNAL FOR BEARING FAULT DIAGNOSIS.

Varun Sharma, Sanjeev Gupta,
Department of ME
GCET, Jammu
J&K, India

S.K Tiwari,
Department of ME
NIT, Jalandhar
Punjab, India

Snehsheel Sharma
Department of ME
KCET, Amritsar
Punjab, India

Abstract—**The present study investigated the use of ensemble empirical mode decomposition (EEMD) based residual signals for the condition monitoring and fault diagnosis in the bearings. The acquired signals were decomposed using EEMD technique to obtain intrinsic mode functions (IMFs). For further processing the sensitive IMFs were selected on the basis of their similarity index with the original signal. The residual signal is then obtained by subtracting the ineffective IMFs from the effective IMFs. After that the five statistical features (namely: Root mean square value (RMS), crest factor (CF), peak-to-RMS (pk2rms), impulse factor (IF) and kurtosis (Ku)) and five entropy based features (namely: Approximate entropy (ApEn), permutation energy (PE), Sample entropy (SampEn), dispersion entropy (DE), and fuzzy entropy (FzEn)) were extracted from residual signal. The extracted features were fed to the two state-of-the-art classifiers, support vector machine (SVM) and random forest (RF) for the classification of different bearing faults. The analysis of results shows that the proposed method has potential for identifying and classifying different bearing's faults**

Keywords—**Vibration analysis, Fault diagnosis, EEMD, Residual signals.**

I. INTRODUCTION

A bearing is a rotating machine element which supports the load, provides relative motion with minimum friction. Rolling contact bearings are also called anti friction bearings and these types of bearings are not suitable for shock loads due to poor damping and balls are subjected to plastic deformation under shock loads leading to noise and vibrations (Tandon and Choudhury, 1999).The health of the machine can be determined by condition monitoring techniques (CMTs).(Jardine et al., 2006).The vibration signal is highly sensitive to bearing status, allowing characteristic information closely related to bearing failure to be extracted. Fourier transform, wavelet transform, and Empirical Mode Decomposition (EMD) are extensively used methods for extracting vibration signal features. EMD has higher signal processing capabilities than the two approaches discussed above, allowing it to effectively analyze signals with more complicated features. It has been observed that EEMD is very promising to denoise the complex machine signals. It is combined with different entropy approach for the machine fault diagnosis. The entropy has been proved as a good indicator to reflect system complexity. But most of the entropy methods are sensitive to selected parameters. In the present study the EEMD is used as denoising techniques and five statistical and five entropy parameters are considered as feature vectors to reflect the condition of the bearing. The efficacy of the proposed methodology is checked by the two state-of-art classifiers: support vector machine (SVM) and random forest.

II. PROPOSED METHODOLOGY

The flowchart describing the experimental methodology is detailed in Fig. 4. First of all, data acquisition of vibration signals from both healthy and damaged bearing was done. Then decomposing and denoising of each the segmented sub-signal was performed using EEMD. Significant IMFs are selected on the basis of their similarity index with original signal based upon the dynamic time wrapping (DTW)

International Journal of Engineering Applied Sciences and Technology, 2025
Vol. 9, Issue 10, ISSN No. 2455-2143, Pages 50-72
Published Online February 2025 in IJEAST (http://www.ijeast.com)

algorithm. Residual signal is obtained by subtracting the sum of ineffective IMFs from the sum of significant IMFs. Statistical features of each of the selected IMF the statistical features are computed. Finally calculated features are used to describe the states of the bearing via classification through RF. Statistical features that better describes the health conditions of the roller bearings were extracted. Adopting the supervised machine learning through classifiers based on SVM and RF raises diagnosis accuracy.

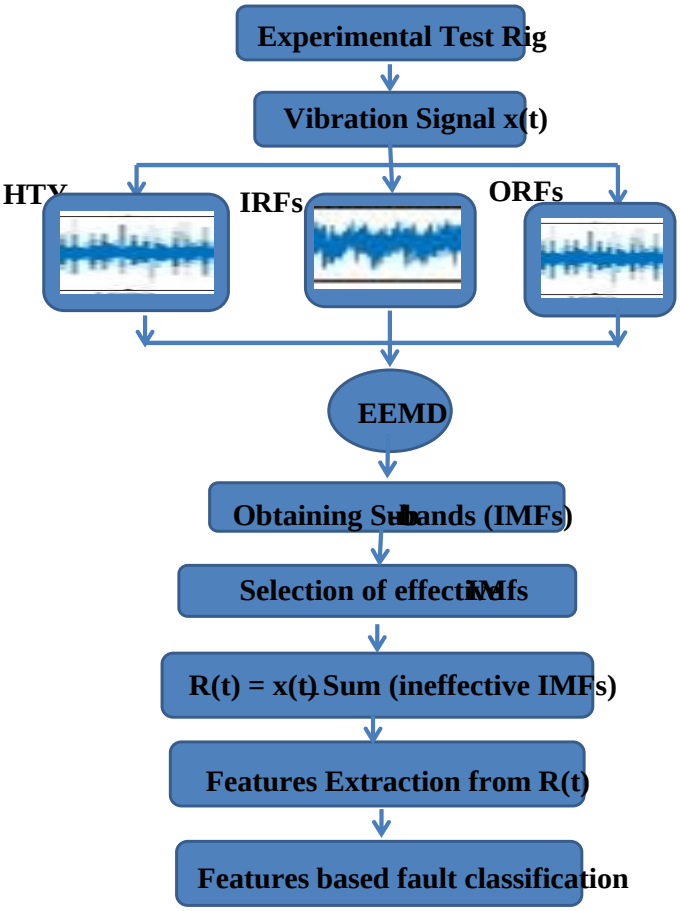

Fig. 1Experimental methodology

III. EXPERIMENTAL TEST RIG

The experimental rig, as shown in Fig.2, is basically an electro-mechanical system. The motor-side bearing is the component under examination.

Fig.2 Bearing test rig

Electro-discharge Machining was used to seed localized defects on inner and outer races, with varying degrees of damage. The point defects with the diameter ranging from 3 to 5 mm were introduced. The bearing was operated at six distinct speeds, ranging from 25 to 50 Hz. The speed's variation, is attained by variable frequency drive (VFD). Data was collected at a sampling rate of 65500 k samples/s. The acquired experimental data is detailed in Table1, where, (i). HTY is data for healthy bearing (ii). IRF is bearing data with inner race fault (iii). ORF is bearing data with outer race fault

International Journal of Engineering Applied Sciences and Technology, 2025
Vol. 9, Issue 10, ISSN No. 2455-2143, Pages 50-72
Published Online February 2025 in IJEAST (http://www.ijeast.com)

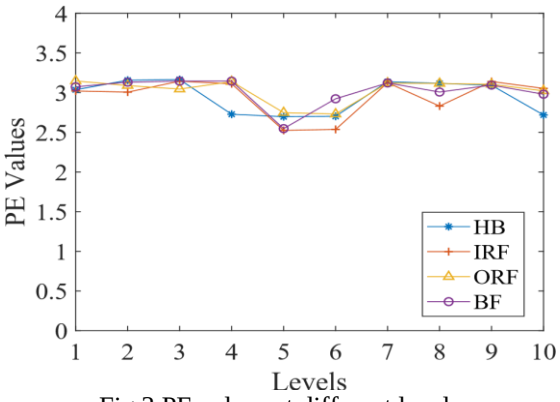

Fig.3 PE values at different levels

Fig.4 Tests bearings with IRF

There are a total of 40 experimental signals that are tabulated in Table1. The 6 signals denote a healthy bearing state, while the 36 signals are acquired for faulty bearing. With a sampling time of 5.2 seconds, 65,536 data points were taken for each recorded signal.

Table -1Experimental conditions (∗ -available data)

Bearing condition	Fault severity (in mm)	Speed (Hz) 25 Hz	30 Hz	35 Hz	40 Hz	45 Hz	50 Hz
HTY	-	∗	∗	∗	∗	∗	∗
IRF	3	∗	∗	∗	∗	∗	∗
	4	∗	∗	∗	∗	∗	∗
	5	∗	∗	∗	∗	∗	∗
ORF	3	∗	∗	∗	∗	∗	∗
	4	∗	∗	∗	∗	∗	∗
	5	∗	∗	∗	∗	∗	∗

IV. EXPERIMENTAL ANALYSIS

In this research work the dynamic response of the system with healthy bearing for different speeds their time–domain representation are obtained and plotted in Figure 5. The time domain graphs for the healthy bearing, with an operating speed of 25-50 Hz, are shown in Fig. 5(a)-(f).With increase in the fault severity the overall vibration amplitude is increased and this increase can be observed from Fig. 6. The figure is plotted for the IR_{Fa} with the fault severity of 3 mm at different operating speeds. Figure 6 (a) is plotted for operating speed of 25 Hz and then plots for the various speeds are obtained in Fig. 6 (b)-(f), respectively. Similar trends can be observed in Figure 7 for the bearings with OR_{Fa} with the fault severity of 3m. Fig. 7(a)-(d) are the time domain representation of signals acquired for the bearing with faulty outer race at variable speed conditions. The impulses in the signal are indicative of the faulty bearing.

International Journal of Engineering Applied Sciences and Technology, 2025
Vol. 9, Issue 10, ISSN No. 2455-2143, Pages 50-72
Published Online February 2025 in IJEAST (http://www.ijeast.com)

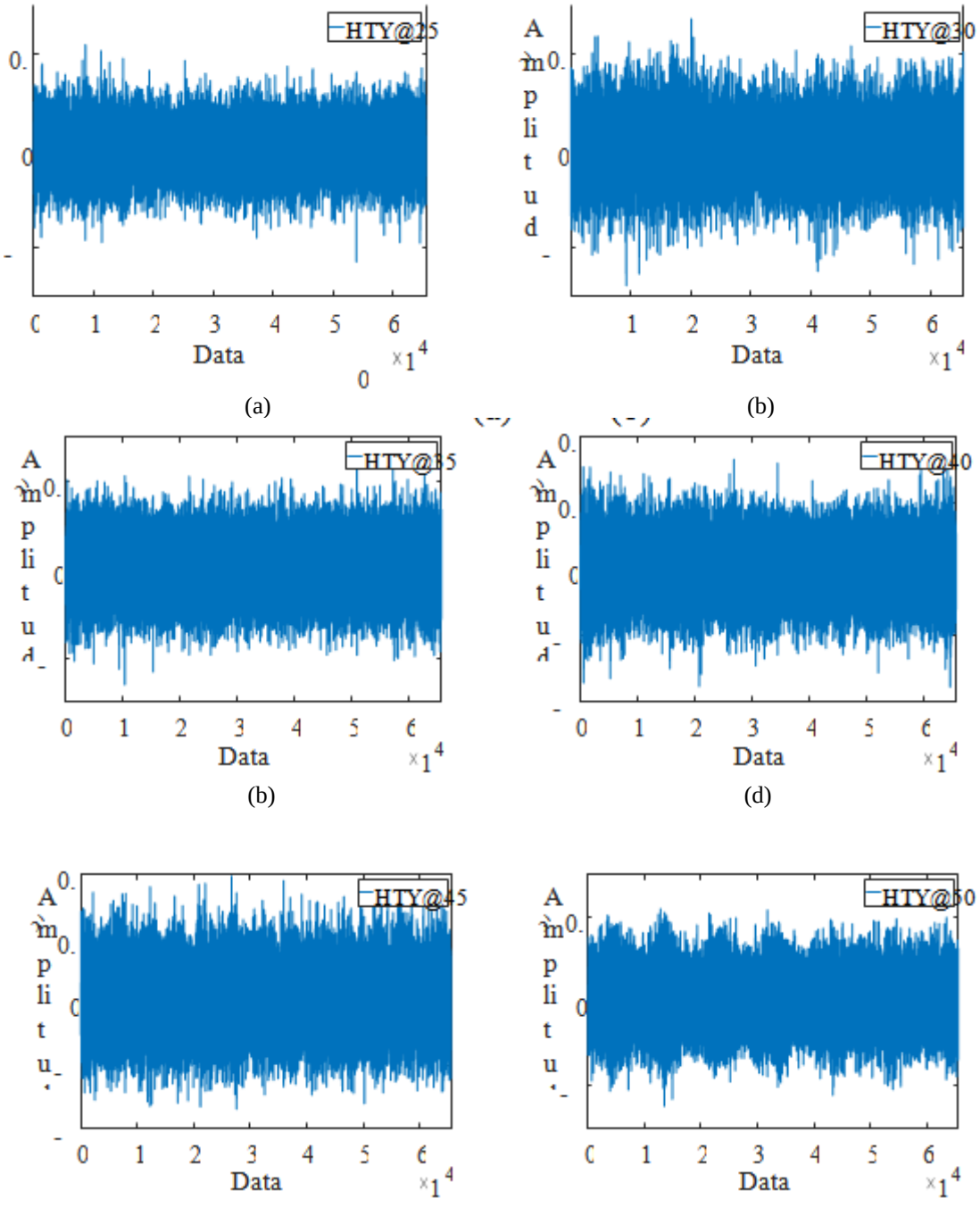

Figure 5: Time domain signals for the healthy bearing at various speeds: (a) 25Hz;(b) 30 Hz; (c) 35 Hz; (d) 40 Hz; (e) 45 Hz, and (f) 50 Hz

International Journal of Engineering Applied Sciences and Technology, 2025
Vol. 9, Issue 10, ISSN No. 2455-2143, Pages 50-72
Published Online February 2025 in IJEAST (http://www.ijeast.com)

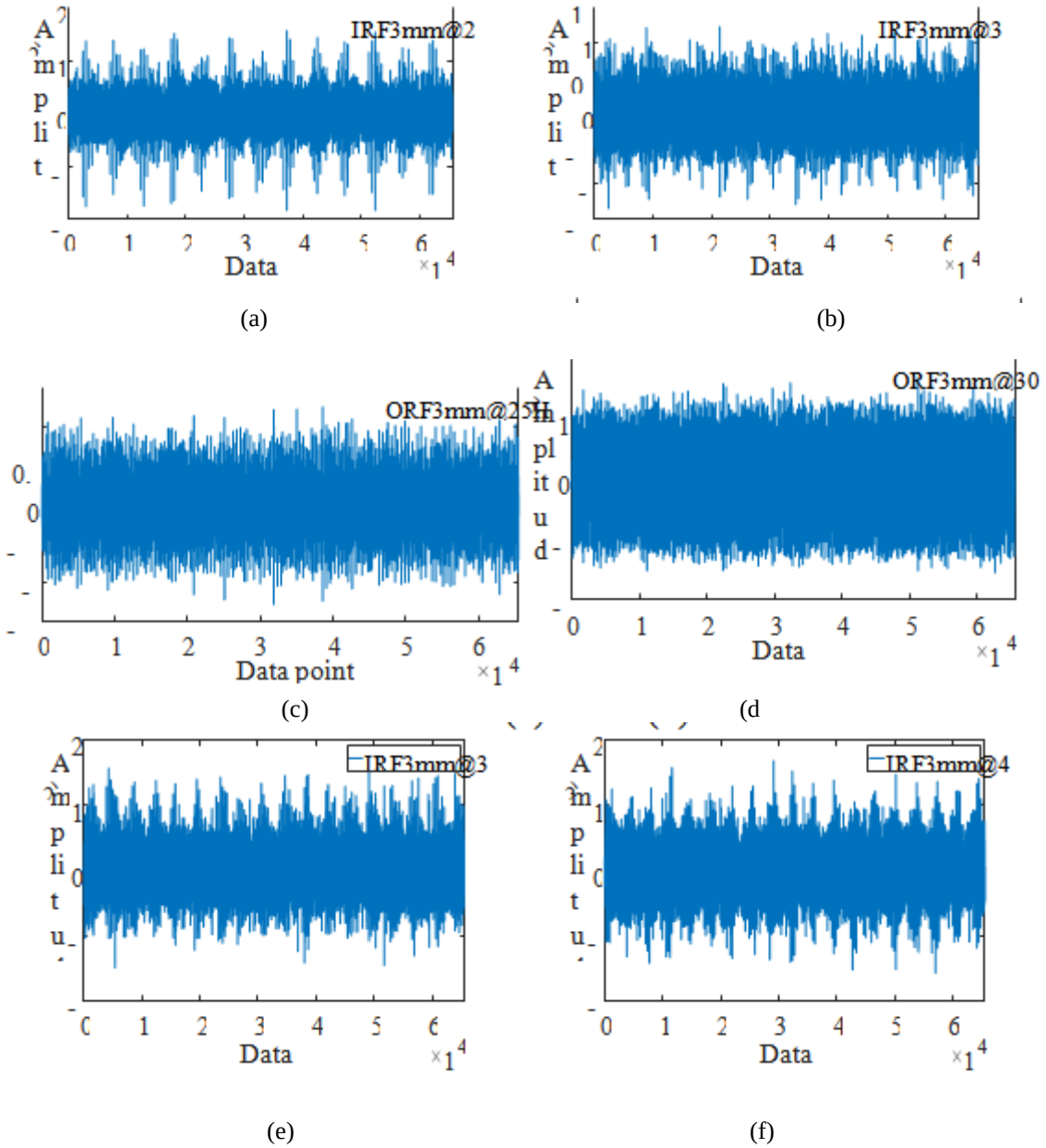

Figure 6: Time domain signals for IRF with the fault size of 3mm: (a) at 25 Hz;(b) at 30 Hz; (c) at 35 Hz; (d) at 40 Hz; (e) at 45 Hz; (f) at 50 Hz

International Journal of Engineering Applied Sciences and Technology, 2025
Vol. 9, Issue 10, ISSN No. 2455-2143, Pages 50-72
Published Online February 2025 in IJEAST (http://www.ijeast.com)

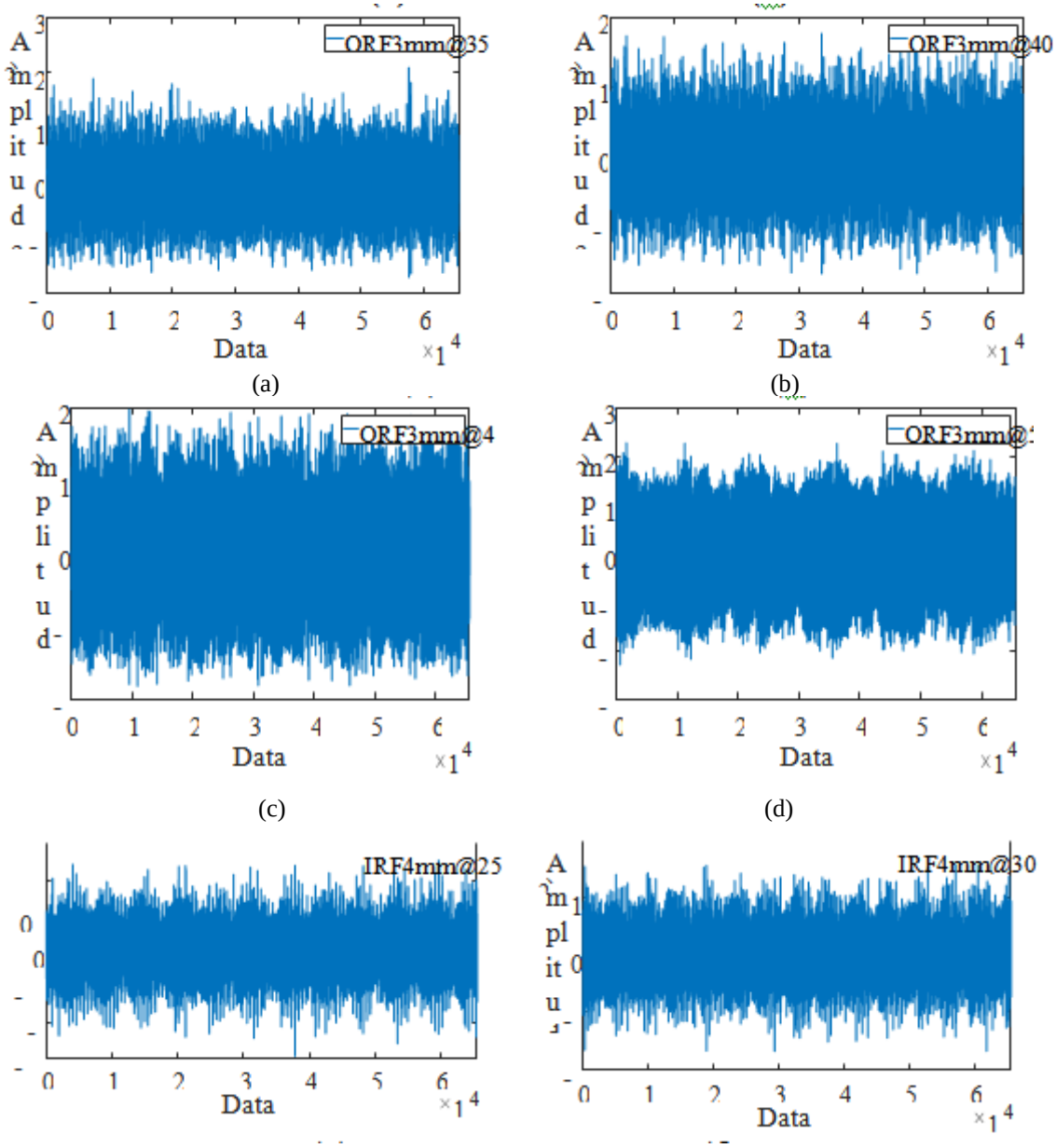

Figure 7: Time domain signals for ORF with the fault size of 3mm: (a) at 30 Hz;(b) at 40 Hz; (c) at 25 Hz; (d) at 30 Hz; (e) at 45 Hz; (f) at 50 Hz

International Journal of Engineering Applied Sciences and Technology, 2025
Vol. 9, Issue 10, ISSN No. 2455-2143, Pages 50-72
Published Online February 2025 in IJEAST (http://www.ijeast.com)

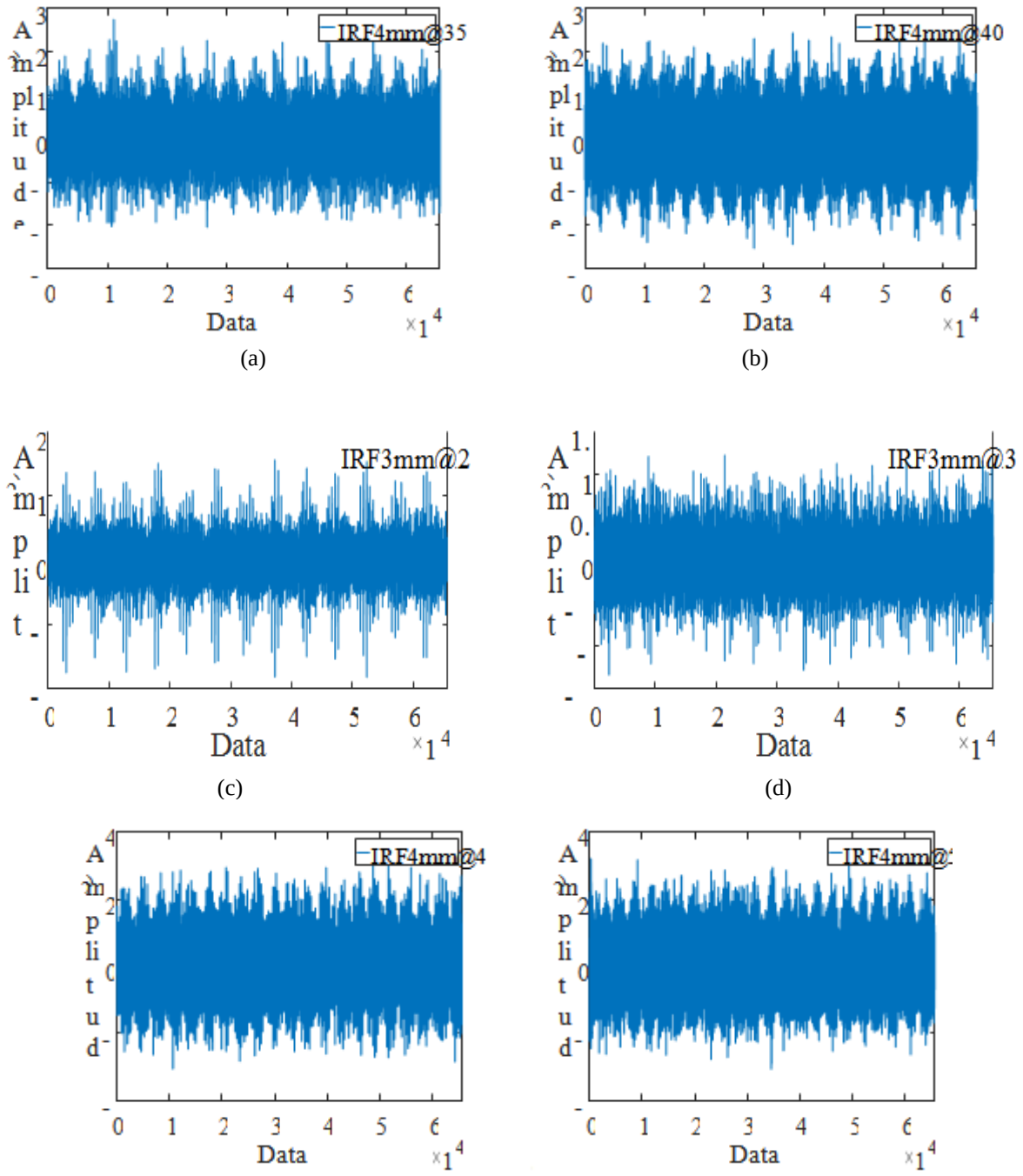

Figure 8: Time domain signals for IRF with the fault size of 4mm: (a) at 25 Hz;(b) at 30 Hz; (c) at 35 Hz; (d) at 40 Hz; (e) at 45 Hz; (f) at 50 Hz

International Journal of Engineering Applied Sciences and Technology, 2025
Vol. 9, Issue 10, ISSN No. 2455-2143, Pages 50-72
Published Online February 2025 in IJEAST (http://www.ijeast.com)

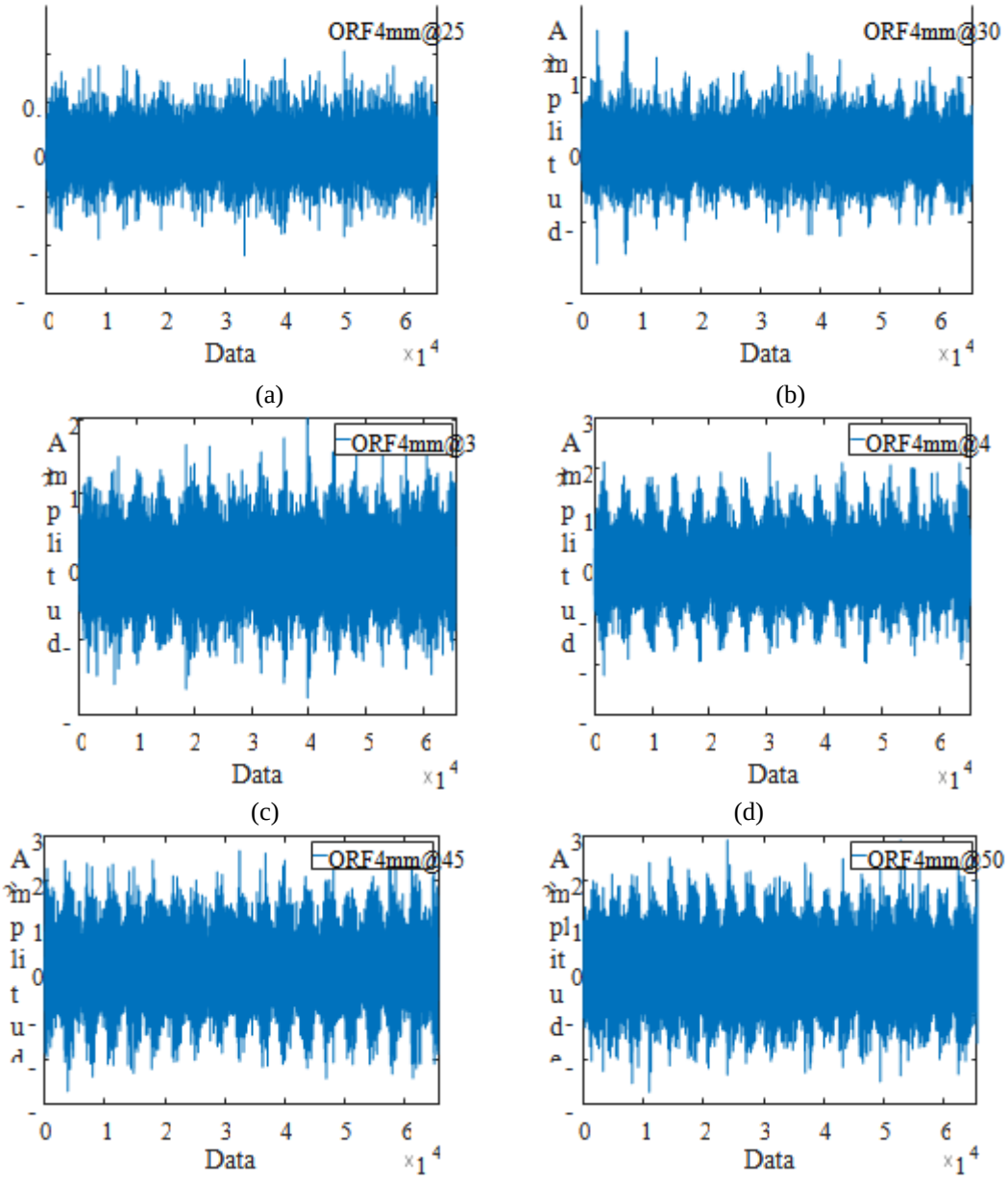

Fig. 9: Time domain signals for ORF with the fault size of 4mm: (a) at 25 Hz;(b) at 30 Hz; (c) at 35 Hz; (d) at 40 Hz; (e) at 45 Hz; (f) at 50 Hz

B. **EEMD on Experimental Signal-**

The acquired machine signals usually have low signal-to-noise ratio (SRN). The SRN of a signal can be enhanced by pre-processing. The pre-processors are usually the electronic filters and decomposes the signal into different sub-bands. The EMD based filters are extensively applied to decompose the acquired machine signals. Many advancement to the conventional EMD algorithm were reported time-to-time by various researchers. One such advancement is the EEMD technique, to overcome mode mixing problem and gives finer results than EMD. The EEMD technique is a powerful tool for non-linear and non-stationary signal analysis.

Each signal reflecting different experimental conditions was first decomposed by EEMD. The decomposed sub-bands are called intrinsic mode functions (IMFs). The various parameters used for the algorithms of EEMD are:

(i). the standard deviation of the additional noise to the standard deviation of the signal is 0.2. (ii). Ensemble number for the EEMD = 120.

International Journal of Engineering Applied Sciences and Technology, 2025
Vol. 9, Issue 10, ISSN No. 2455-2143, Pages 50-72
Published Online February 2025 in IJEAST (http://www.ijeast.com)

Features extraction: In the present study five statistical and five entropy features are extracted from the residual signal. The detail of them are: Statistical features (a) Root mean square value (RMS), (b) Kurtosis (Ku), (c) Standard Deviation (SD), (d) Impulse factor (IF), (e) Peak-to-RMS (pk2rms). Entropy features (a) Approximate Entropy (ApEn), (b) Sample Entropy (SampEn), (c) Fuzzy Entropy (FzEn), (d) Permutation Entropy (PE), (e) Dispersion Entropy (DE).

C. EEMD of signals acquired for healthy bearing

Decomposition levels for healthy bearing at different operating speeds are given in Figure 10 (a-f).

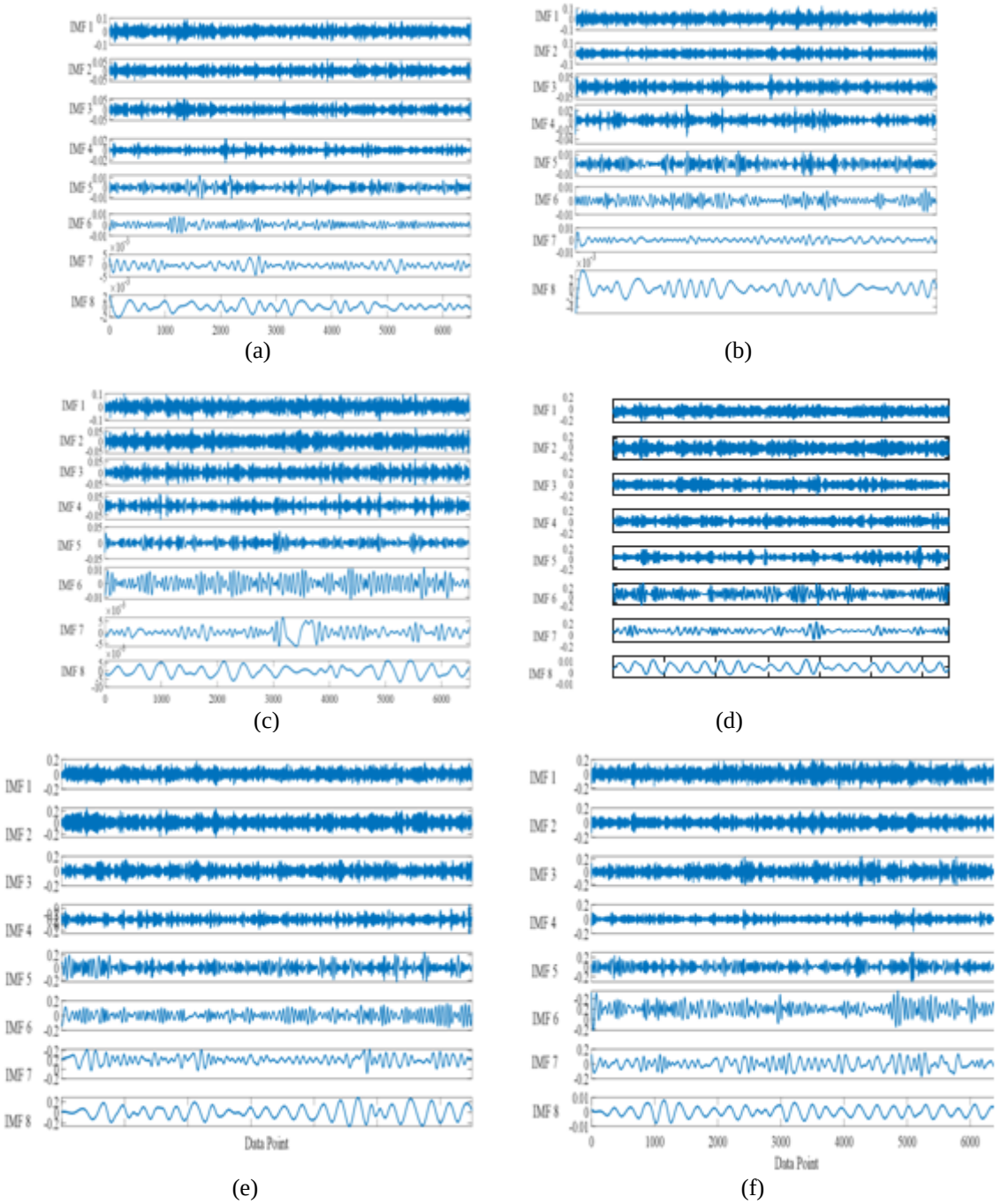

Fig.10 IMF decomposition obtained through EEMD of Healthy bearing signals:(a)25 Hz; (b) 30 Hz; (c) 35 Hz; (d) 40 Hz; (e) 45 Hz; and (f) 50 Hz

International Journal of Engineering Applied Sciences and Technology, 2025
Vol. 9, Issue 10, ISSN No. 2455-2143, Pages 50-72
Published Online February 2025 in IJEAST (http://www.ijeast.com)

D.**EEMD on signals acquired of bearings with IRF-**

Decomposition levels of bearing with IRF, for the fault severity of 3 mm, 4mm and 5mm at different operating conditions are given in Fig 11, Fig12 and Fig.13 respectively.

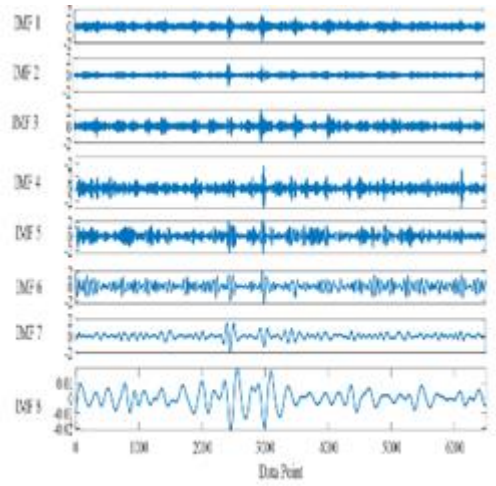

(a)

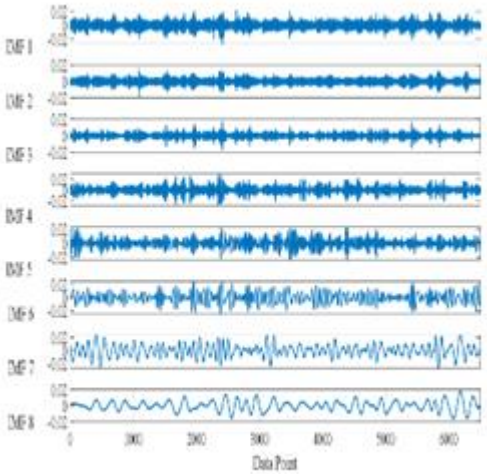

(b)

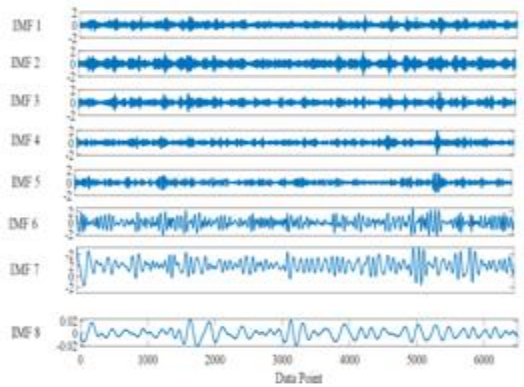

(c)

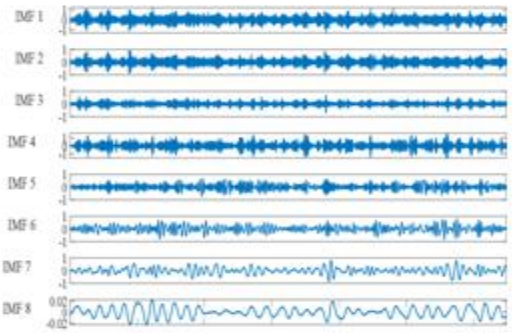

(d)

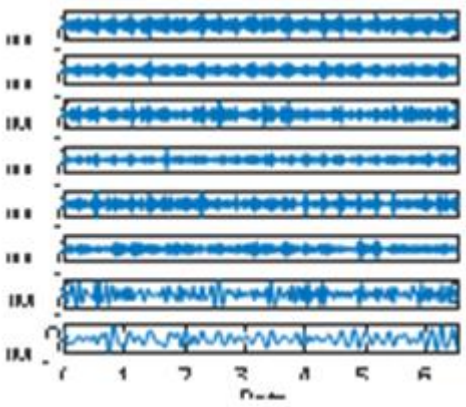

(e)

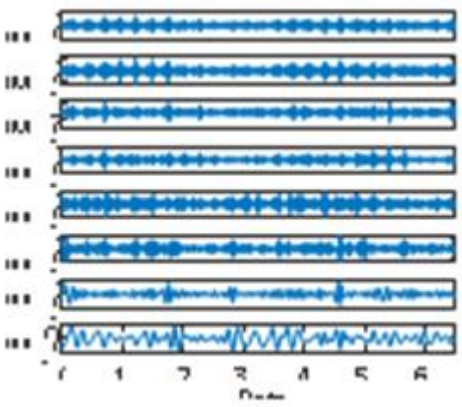

(f)

Fig. 11 IMF decomposition obtained through EEMD of bearing's with IRF of3mm, at: (a) 25 Hz; (b) 30 Hz; (c) 35 Hz; (d) 40 Hz; (e) 45 Hz; and (f) 50 Hz

International Journal of Engineering Applied Sciences and Technology, 2025
Vol. 9, Issue 10, ISSN No. 2455-2143, Pages 50-72
Published Online February 2025 in IJEAST (http://www.ijeast.com)

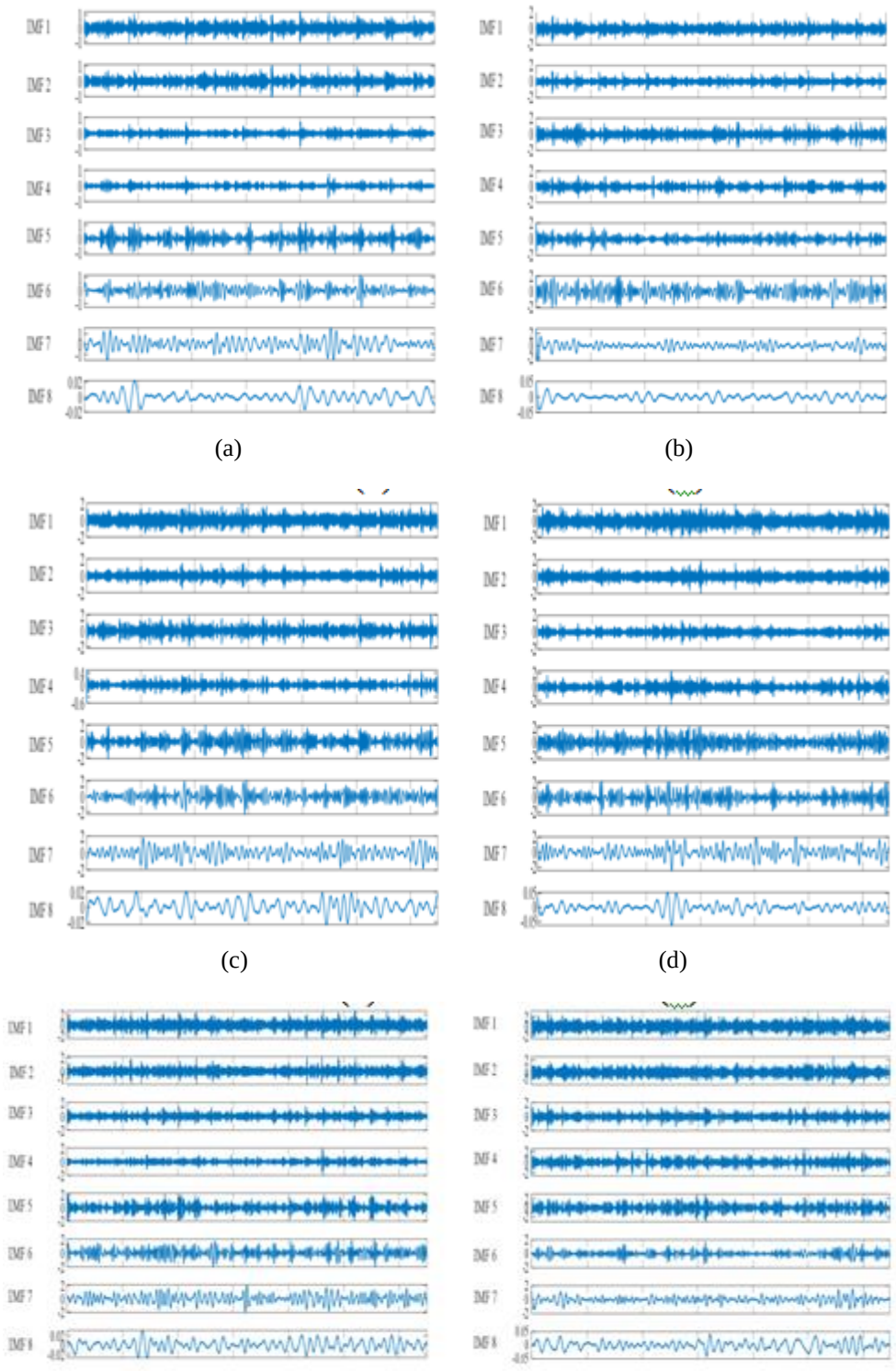

(a) (b)

(c) (d)

(e) (f)

Fig.12IMF decomposition obtained through EEMD of bearing's with IRF of4mm, at: (a) 25 Hz; (b) 30 Hz; (c) 35 Hz; (d) 40 Hz; (e) 45 Hz; and (f) 50 Hz

International Journal of Engineering Applied Sciences and Technology, 2025
Vol. 9, Issue 10, ISSN No. 2455-2143, Pages 50-72
Published Online February 2025 in IJEAST (http://www.ijeast.com)

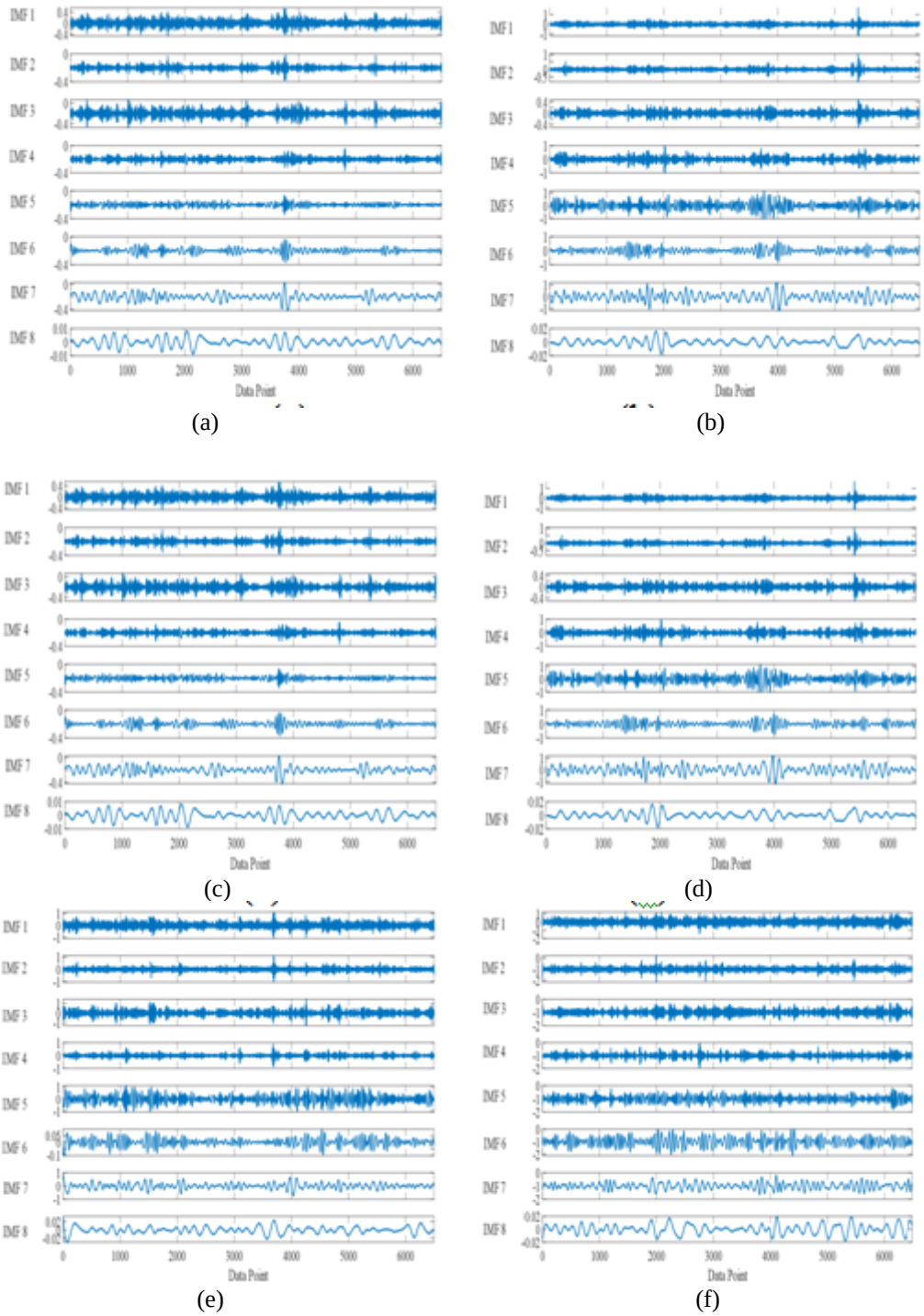

Fig. 13IMF decomposition obtained through EEMD of bearing's with IRF of5mm, at: (a) 25 Hz; (b) 30 Hz; (c) 35 Hz; (d) 40 Hz; (e) 45 Hz; and (f) 50 Hz

International Journal of Engineering Applied Sciences and Technology, 2025
Vol. 9, Issue 10, ISSN No. 2455-2143, Pages 50-72
Published Online February 2025 in IJEAST (http://www.ijeast.com)

E.**EEMD on signals acquired of bearings with ORF-**

Decomposition levels of bearing with ORF, for the fault severity of 3 mm, 4mm and 5mm at different operating conditions are given in Fig. 14, Fig.15 and Fig.16 respectively.

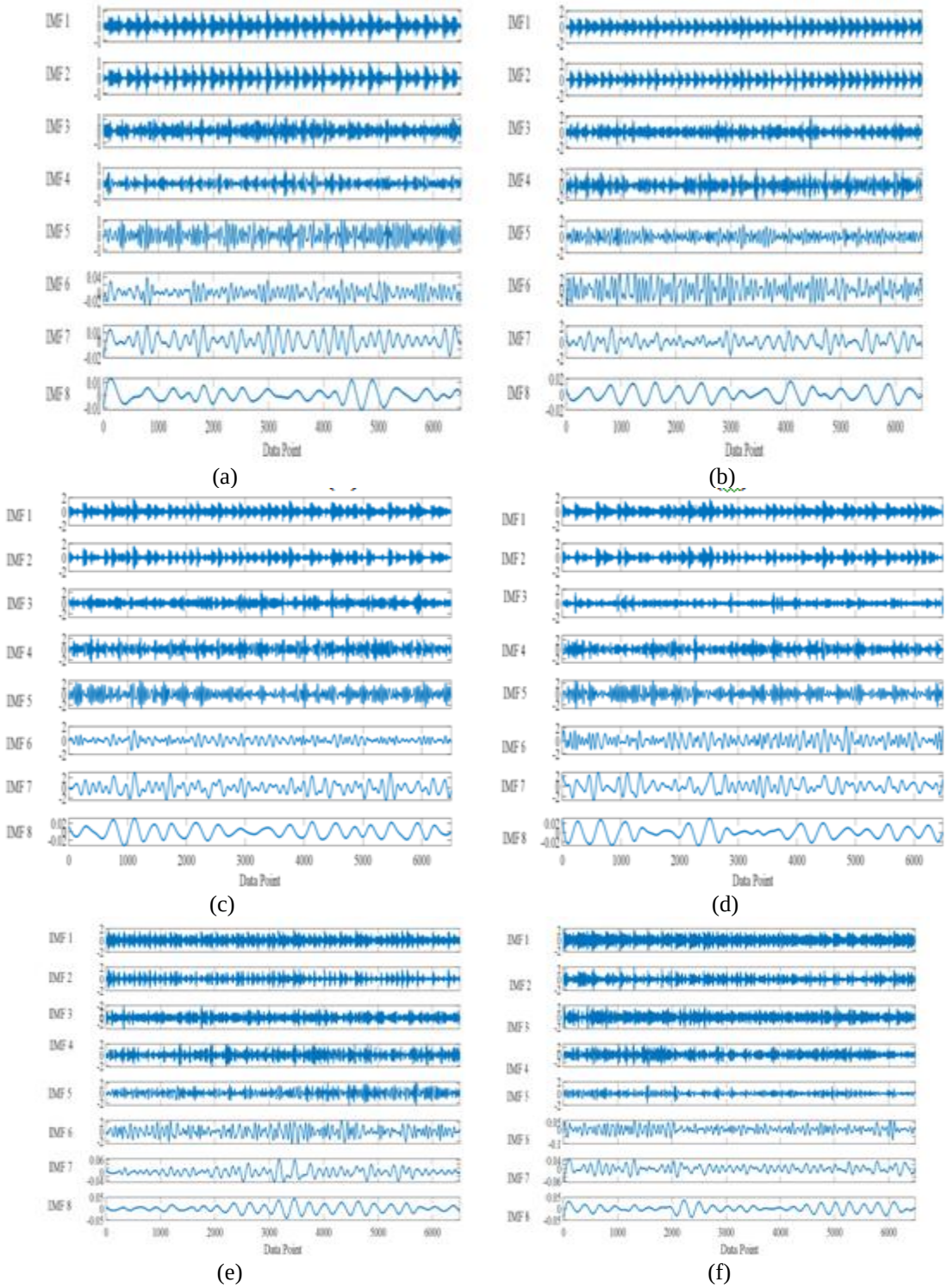

Fig. 14 IMF decomposition obtained through EEMD of bearing's with ORF of3mm, at: (a) 25 Hz; (b) 30 Hz; (c) 35 Hz; (d) 40 Hz; (e) 45 Hz; and (f) 50 Hz

International Journal of Engineering Applied Sciences and Technology, 2025
Vol. 9, Issue 10, ISSN No. 2455-2143, Pages 50-72
Published Online February 2025 in IJEAST (http://www.ijeast.com)

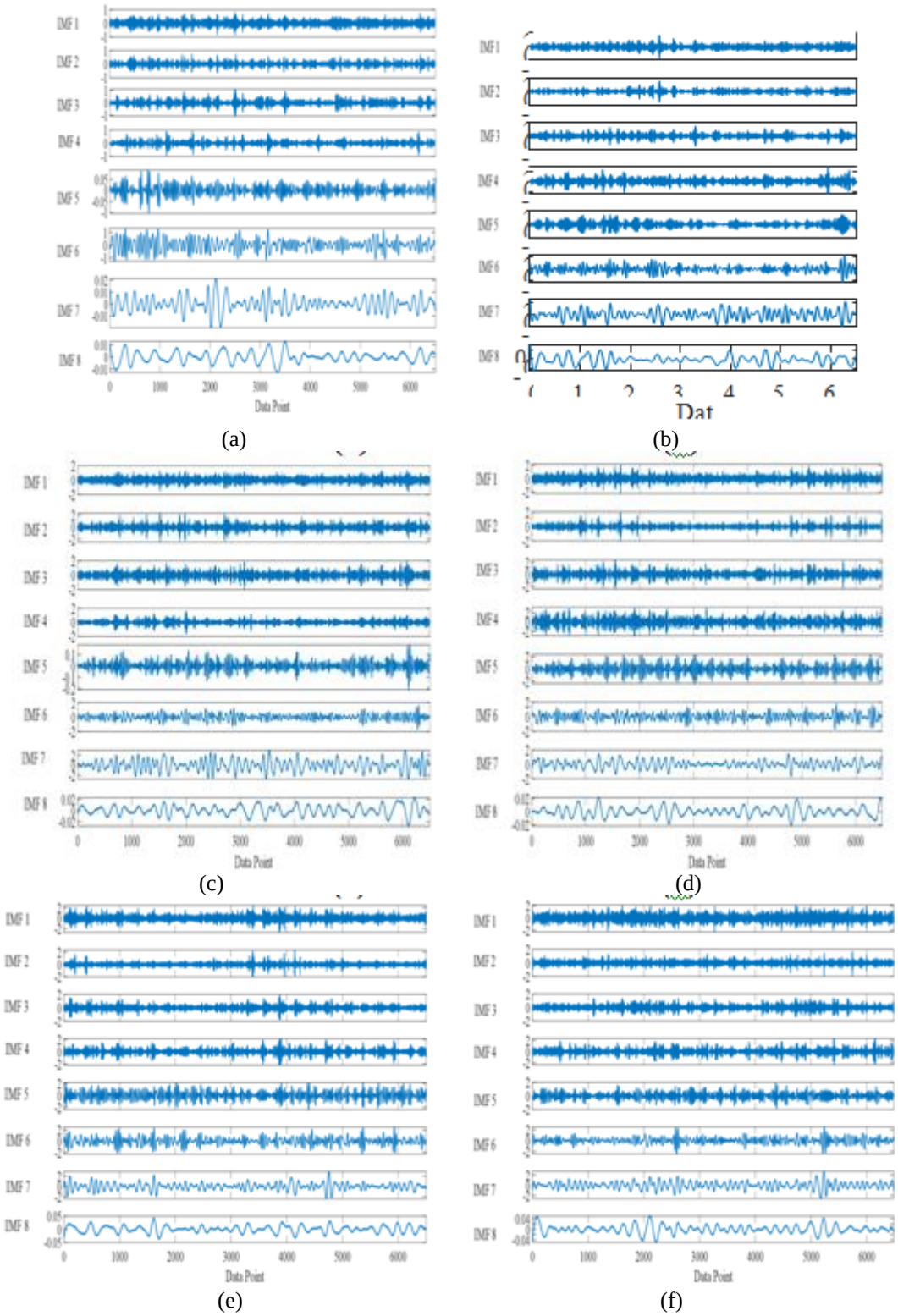

Fig. 15 IMF decomposition obtained through EEMD of bearing's with ORF of 4mm, at: (a) 25 Hz; (b) 30 Hz; (c) 35 Hz; (d) 40 Hz; (e) 45 Hz; and (f) 50 Hz

International Journal of Engineering Applied Sciences and Technology, 2025
Vol. 9, Issue 10, ISSN No. 2455-2143, Pages 50-72
Published Online February 2025 in IJEAST (http://www.ijeast.com)

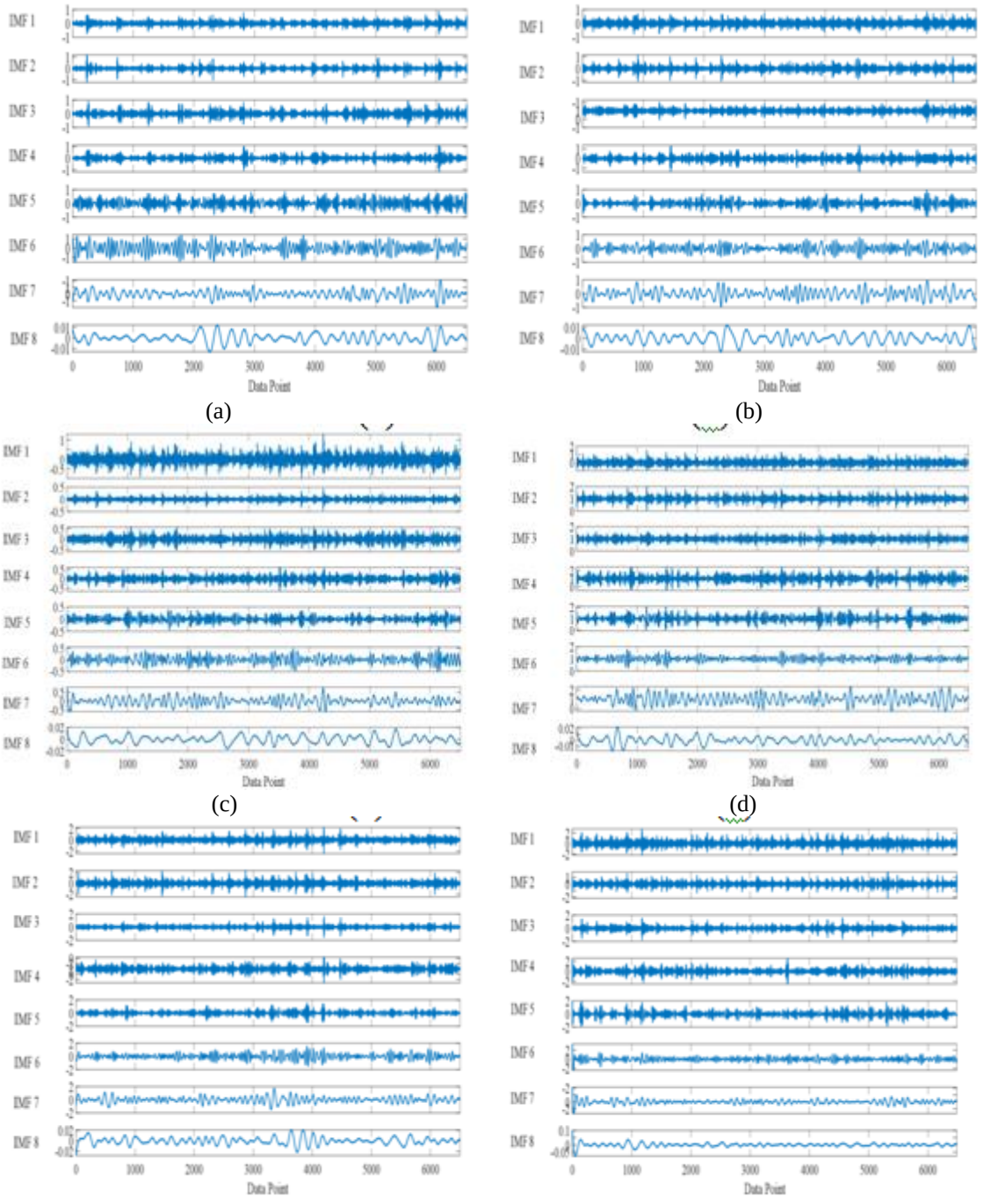

Fig. 16IMF decomposition obtained through EEMD of bearing's with ORF of 5mm, at: (a) 25 Hz; (b) 30 Hz; (c) 35 Hz; (d) 40 Hz; (e) 45 Hz; and (f) 50 Hz

In the present study, the residual signals are obtained by subtracting the sum of insignificant IMFs from the original signals. The selection of significant IMFs is based upon their similarity index obtained using DTW algorithm. Five-statistical and five entropy features are extracted as the input features. These features are used to train and test two classifiers based on "support vector machine (SVM) and random forest (RF)" to detect the fault type in the bearing.

$$R(t) = x(t) - \text{sum(insignificant IMFs)} \quad (1)$$

The statistical and entropy-based feature values for the residual signal of healthy bearing, acquired at different speeds, are computed and tabulated. Table 2 can be referred for

International Journal of Engineering Applied Sciences and Technology, 2025
Vol. 9, Issue 10, ISSN No. 2455-2143, Pages 50-72
Published Online February 2025 in IJEAST (http://www.ijeast.com)

statistical feature values of healthy bearing running at different speeds. The values of different entropy-based features, calculated at different operating conditions can be observed from Table.4

Table- 4 Statistical features: Extracted from EEMD based residual signal of healthy bearing

Bearing condition	Feature vector	Speed					
		$25Hz$	$30Hz$	$35Hz$	$40Hz$	$45Hz$	$50Hz$
HTY	RMS	0.0703	0.0784	1.4761	3.2491	3.9743	3.1684
	Ku	2.0369	2.0354	2.9803	3.0461	3.0938	3.0067
	IF	0.0270	0.0270	5.0465	5.4429	4.0796	4.0675
	SD	0.0349	0.0349	5.6266	4.7894	4.9605	5.0256
	$pk2rms$	0.0198	0.0163	3.6021	4.8367	3.8161	3.5634

Table- 5: Entropy features: Extracted from EEMD based residual signal of healthy bearing

Bearing condition	Feature vector	Speed					
		$25Hz$	$30Hz$	$35Hz$	$40Hz$	$45Hz$	$50Hz$
HTY	$ApEn$	0.0122	0.0343	0.7684	0.7876	0.9553	0.9893
	$SampEn$	1.3206	2.6580	2.6748	2.9847	2.9957	2.8974
	$FzEn$	0.2267	0.6743	4.7664	5.0006	4.9963	4.8746
	PE	2.9958	2.8956	3.9967	3.7894	3.0001	3.9887
	DE	1.1078	1.5012	2.9711	2.8858	2.9012	2.8947

After extracting the statistical and entropy features from the residual signal of healthy bearing at different speeds, the feature extraction is done for the bearings with inner race faults. The both statistical and entropy-based features were extracted for different types of IRFs at different operating conditions. The values of the different statistical and Entropy features obtained for the fault size of 3mm, 4mm and 5mm, are tabulated in Table 4, Table 5, Table 6, Table7, Table8 and Table 9 respectively.

Bearing condition	Feature vector	Speed					
		$25Hz$	$30Hz$	$35Hz$	$40Hz$	$45Hz$	$50Hz$
IRF (3 mm)	RMS	1.4879	2.6034	4.0143	4.5863	5.0066	5.9403
	Ku	5.9875	6.0034	7.9001	7.6687	6.9889	7.9976
	IF	3.2176	3.8791	5.0997	5.9044	6.1117	6.7836
	SD	3.7893	3.6988	5.7743	6.7894	7.5069	8.6725
	$pk2rms$	3.8235	3.8965	4.6654	5.8777	6.1234	5.9054

Table-6 Statistical features: Extracted from EEMD based residual signal of bearing with IRF (for the fault severity of 3 mm) at different speeds

International Journal of Engineering Applied Sciences and Technology, 2025
Vol. 9, Issue 10, ISSN No. 2455-2143, Pages 50-72
Published Online February 2025 in IJEAST (http://www.ijeast.com)

Bearing condition	Feature vector	Speed					
		$25Hz$	$30Hz$	$35Hz$	$40Hz$	$45Hz$	$50Hz$
IRF (4mm)	RMS	2.3370	4.9874	5.3678	6.0021	6.7453	7.8711
	Ku	2.5646	2.7856	4.6540	6.7776	7.5465	8.6232
	IF	1.6671	1.4720	4.7845	5.7721	4.9990	4.5799
	SD	4.7856	6.1511	6.5655	7.0023	7.1237	8.8895
	$pk2rms$	4.6730	4.0300	5.3146	4.6692	4.6649	4.5571

Table-7 Statistical features: Extracted from EEMD based residual signal of bearing with IRF (for the fault severity of 4 mm) at different speeds

Bearing condition	Feature vector	Speed					
		$25Hz$	$30Hz$	$35Hz$	$40Hz$	$45Hz$	$50Hz$
IRF (5 mm)	RMS	5.7056	6.8890	9.8978	8.6645	9.0067	9.5677
	Ku	7.8865	8.0062	8.9886	9.4589	9.1123	9.1008
	IF	1.1342	2.0010	5.5675	5.6675	6.1157	6.8815
	SD	3.4562	3.0034	5.1254	6.7781	6.7321	7.7659
	$pk2rms$	3.4451	4.5567	5.8757	4.1259	4.8278	4.7590

Table-8: Statistical features: Extracted from EEMD based residual signal of bearing with IRF (for the fault severity of 5 mm) at different speeds

Bearing condition	Feature vector	Speed					
		$25Hz$	$30Hz$	$35Hz$	$40Hz$	$45Hz$	$50Hz$
IRF (3 mm)	$ApEn$	0.6574	0.7075	0.7689	0.8237	0.9758	0.9995
	$SampEn$	3.7904	3.7566	4.8764	4.9993	5.9037	5.8865
	$FzEn$	1.7745	1.8761	4.9984	6.9073	6.9878	7.5763
	PE	4.3876	4.9986	7.0043	6.8967	7.1298	7.9762
	DE	3.3345	3.1205	4.9865	5.9876	5.7756	6.8790

Statistical and entropy-based features were extracted for different types of ORFs at different operating conditions. The values of the different statistical and entropy features obtained for the fault size of 3mm, 4mm and 5mm, are tabulated in Table 10, Table 11, Table 12, Table13, Table14 and Table 15, respectively.

International Journal of Engineering Applied Sciences and Technology, 2025
Vol. 9, Issue 10, ISSN No. 2455-2143, Pages 50-72
Published Online February 2025 in IJEAST (http://www.ijeast.com)

Table-9 Entropy features: Extracted from EEMD based residual signal of bearing with IRF (for the fault severity of 5 mm) at different speeds

Bearing condition	Feature vector	Speed					
		$25Hz$	$30Hz$	$35Hz$	$40Hz$	$45Hz$	$50Hz$
ORF (3 mm)	RMS	2.1035	2.5569	3.7839	5.8743	6.4598	7.7782
	Ku	5.6743	6.5603	7.1456	7.9754	9.2940	9.4006
	IF	4.5535	4.3070	4.8665	4.7789	7.4451	7.5476
	SD	3.2398	3.5582	5.9751	6.7845	7.0094	7.8965
	$pk2rms$	4.0331	4.9301	4.1111	5.7825	6.0048	7.8954

Table -10: Statistical features: Extracted from EEMD based residual signal of bearing with ORF (for the fault severity of 3 mm) at different speeds

Bearing condition	Feature vector	Speed					
		$25Hz$	$30Hz$	$35Hz$	$40Hz$	$45Hz$	$50Hz$
ORF (4mm)	RMS	4.4589	4.8540	5.5948	7.1231	7.0080	7.9841
	Ku	3.1104	3.6548	4.8814	6.6593	7.0049	8.9975
	IF	2.9452	3.1231	4.5569	4.9867	5.0076	5.3256
	SD	5.9854	6.4872	7.8353	8.4671	8.1263	8.0009
	$pk2rms$	5.1190	5.0500	5.5111	5.5464	5.0830	6.6784

Table -11: Statistical features: Extracted from EEMD based residual signal of bearing with ORF (for the fault severity of 4 mm) at different speeds

Bearing condition	Feature vector	Speed					
		$25Hz$	$30Hz$	$35Hz$	$40Hz$	$45Hz$	$50Hz$
ORF (5 mm)	RMS	6.8874	6.7804	9.0112	9.0003	9.5431	9.9987
	Ku	8.8978	8.7624	8.8769	9.3986	9.2276	9.7839
	IF	2.3568	2.9836	5.8793	5.9982	6.8673	7.0108
	SD	4.6521	4.5756	5.6573	5.9006	6.9981	8.6705
	$pk2rms$	5.6742	5.5678	6.4034	6.7780	6.1450	6.9003

Table- 12: Statistical features: Extracted from EEMD based residual signal of bearing with ORF (for the fault severity of 5 mm) at different speeds

International Journal of Engineering Applied Sciences and Technology, 2025
Vol. 9, Issue 10, ISSN No. 2455-2143, Pages 50-72
Published Online February 2025 in IJEAST (http://www.ijeast.com)

Bearing condition	Feature vector	Speed					
		$25Hz$	$30Hz$	$35Hz$	$40Hz$	$45Hz$	$50Hz$
ORF (3 mm)	$ApEn$	0.7543	0.7869	0.9659	0.9093	0.9652	0.9767
	$SampEn$	3.6654	3.9063	5.6211	6.0099	6.6078	6.9004
	$FzEn$	3.6759	4.0179	4.4467	5.6303	5.9076	5.0950
	PE	2.2008	2.4405	3.1108	3.2085	3.9573	4.0405
	DE	6.0039	6.0491	5.9909	7.9067	7.9111	7.8460

Table 13: Entropy features: Extracted from EEMD based residual signal of bearing with ORF (for the fault severity of 3 mm) at different speeds

Bearing condition	Feature vector	Speed					
		$25Hz$	$30Hz$	$35Hz$	$40Hz$	$45Hz$	$50Hz$
ORF (4mm)	RMS	4.4589	4.8540	5.5948	7.1231	7.0080	7.9841
	Ku	3.1104	3.6548	4.8814	6.6593	7.0049	8.9975
	IF	2.9452	3.1231	4.5569	4.9867	5.0076	5.3256
	SD	5.9854	6.4872	7.8353	8.4671	8.1263	8.0009
	$pk2rms$	5.1190	5.0500	5.5111	5.5464	5.0830	6.6784

Table 14: Entropy features: Extracted from EEMD based residual signal of bearing with ORF (for the fault severity of 4 mm) at different speeds

Bearing condition	Feature vector	Speed					
		$25Hz$	$30Hz$	$35Hz$	$40Hz$	$45Hz$	$50Hz$
ORF (5 mm)	$ApEn$	0.8967	0.8978	0.9954	0.9817	0.9899	0.9877
	$SampEn$	3.3435	3.5670	6.6741	7.1457	7.8506	7.9804
	$FzEn$	3.5645	3.5611	4.9867	5.7141	6.6458	6.8745
	PE	2.9096	2.9984	3.7060	3.0718	3.8891	5.6785
	DE	6.7083	7.8650	9.4795	9.5601	9.1239	8.9564

Two types of bearing faults with different degree of damage were considered in the present study: Inner race fault, outer race fault. For each type of fault, its size was varied from 3 mm to 5 mm with an intermittent fault size of 4 mm.
For Group-I, the features for healthy bearings and IRFs with various degrees of damage at various speeds were considered. Thus Group-I contain 60 features extracted from the residual signal of healthy bearing and 180 features extracted from the bearings with IRF damages. Total number of features in Group-I is thus 240. Table 16 show the accuracy obtained with both of the classifiers.

International Journal of Engineering Applied Sciences and Technology, 2025
Vol. 9, Issue 10, ISSN No. 2455-2143, Pages 50-72
Published Online February 2025 in IJEAST (http://www.ijeast.com)

For Group-II, the data for healthy bearing (60 features) and ORFs (180 features) with various degrees of damage at various speeds were considered. Table 17show the accuracy with both the machine learning tools.
For Group-III, the data for IRFs (180 features) and ORFs (180 features) with various degrees of damage at various speeds were considered. Table 18show the accuracy with both the classifiers.
For Group-IV, the data for healthy bearing (60 features), IRFs (180 features), and ORFs (180 features) with various degrees of damage at various speeds were considered. Table 19 show the accuracy with both the classifiers.

Table -15 Groups for classification ('√' included data and '-' data not included)

Group number	Type of data		
	HTY	IRF	ORF
G-I	√	√	-
G-II	√	-	√
G-III	-	√	√
G-IV	√	√	√

Table- 16: Classification accuracy for Group I

Group Number	Total samples	Tested samples	Accuracy	
			SVM	RF
G-I	240	96	95	96

Table- 17 Classification accuracy for Group II

Group Number	Total samples	Tested samples	Accuracy	
			SVM	RF
G-II	240	96	97	98

Table -18 Classification accuracy for Group III

Group Number	Total samples	Tested samples	Accuracy	
			SVM	RF
G-III	360	144	98	98

Table -19 Classification accuracy for Group IV

Group Number	Total samples	Tested samples	Accuracy	
			SVM	RF
G-IV	420	168	99	98

V. CONCLUSION

Based on ensemble empirical mode decomposition (EEMD) residual signals, this study presents an effective method for fault detection in the roller bearings. In the present study, the EEMD is used to pre-process the acquired bearing vibration signals. The sensitive intrinsic mode functions (IMFs) are selected on the basis of their similarity index value computed by applying the dynamic time wrapping algorithm. The bearing health conditions are then identified using five statistical and five entropy based features extracted from the residual signal and fed into two state-of-the-art classifiers, "support vector machine (SVM) and random forest (RF)". The results of the diagnosis show that the proposed method is capable of reliably identifying various types of bearing defects.It can be stated that EEMD based residual signals can be used to achieve a good fault recognition accuracy. It accurately detects the various sorts of bearing defects.

VI. REFERENCE

[1] Tandon, A., & Choudhury, A. (1999). A review of vibration and acoustic measurement methods for the detection of defects in rolling element bearings. Tribology International, 32(6), 469-480.

[2] Jardine, A. K., Lin, D., & Banjevic, D. (2006). A review on machinery diagnostics and prognostics implementing condition-based maintenance. Mechanical Systems and Signal Processing, 20(7), 1483-1510.

[3] McInerny, S. A., & Dai, Y. (2003). Basic vibration signal processing for bearing fault detection. IEEE Transactions on Education, 46(2), 149-156.

[4] Duan, Z., Wu, T., Guo, S., Shao, T., Malekian, R., & Li, Z. (2018). Development and trend of condition monitoring and fault diagnosis of multi-sensors information fusion for rolling bearings: A review. The International Journal of Advanced Manufacturing Technology, 96(1-4), 803-819.

[5] Tandon, N. (1994). A comparison of some vibration parameters for the condition monitoring of rolling element bearings. Measurement, 12(3), 285-289.

[6] Roberts, T., & Talebzadeh, M. (2003). Acoustic emission monitoring of fatigue crack propagation. Journal of Constructional Steel Research, 59(6), 695-712.

[7] Rastegari, A., Archenti, A., & Mobin, M. (2017). Condition based maintenance of machine tools: Vibration monitoring of spindle units. In 2017 Annual Reliability and Maintainability Symposium (RAMS) (pp. 1-6). IEEE.

[8] McFadden, P., & Smith, J. (1983). The vibration produced by a single point defect on the inner race of a rolling element bearing under radial load. University of Cambridge Engineering Department.

[9] McFadden, P. (2000). Detection of gear faults by decomposition of matched differences of vibration signals. Mechanical Systems and Signal Processing, 14(6), 805-817.

[10] Kıral, Z., & Karagulle, H. (2006). Vibration analysis of rolling element bearings with various defects under the action of an unbalanced force. Mechanical Systems and Signal Processing, 20(7), 1967-1991.

[11] Leite, G. d. N. P., Araújo, A. M., Rosas, P. A. C., Stosic, T., & Stosic, B. (2019). Entropy measures for early detection of bearing faults. Physica A: Statistical Mechanics and Its Applications, 514, 458-472.

[12] Yu, D., Cheng, J., & Yang, Y. (2005). Application of EMD method and Hilbert spectrum to the fault diagnosis of roller bearings. Mechanical Systems and Signal Processing, 19(2), 259-270.

[13] Cheng, J., Yu, D., & Yang, Y. (2006). Research on the intrinsic mode function (IMF) criterion in EMD method. Mechanical Systems and Signal Processing, 20(4), 817-824.

[14] Yu, Y., Cheng, J., Yang, Y., & Junsheng, C. (2006). A roller bearing fault diagnosis method based on EMD energy entropy and ANN. Journal of Sound and Vibration, 294(3-5), 269-277.

[15] Du, Q., & Yang, S. (2007). Application of the EMD method in the vibration analysis of ball bearings. Mechanical Systems and Signal Processing, 21(3), 2634-2644.

[16] Cheng, J., Yu, D., Tang, J., & Yang, Y. (2008). Application of frequency family separation method based upon EMD and local Hilbert energy spectrum method to gear fault diagnosis. Mechanism and Machine Theory, 43(6), 712-723.

[17] Li, H., Liu, T., Wu, X., & Chen, Q. (2019). Application of EEMD and improved frequency band entropy in

bearing fault feature extraction. ISA Transactions, 88, 170-185.

[18] Huang, Y., Yang, L., Liu, S., & Wang, G. (2019). Multi-step wind speed forecasting based on ensemble empirical mode decomposition, long short-term memory network and error correction strategy. Energies, 12(9), 1822

[19] Li, C., Zheng, J., Pan, H., Tong, J., & Zhang, Y. (2019). Refined composite multivariate multiscale dispersion entropy and its application to fault diagnosis of rolling bearing. IEEE Access, 7, 47663-47673.

[20] Han, T., Liu, Q., Zhang, L., & Tan, A. C. (2019). Fault feature extraction of low-speed roller bearing based on Teager energy operator and CEEMD. Measurement, 138, 400-408.

[21] Zhan, L., Ma, F., Zhang, J., Li, C., Li, Z., & Wang, T. (2019). Fault feature extraction and diagnosis of rolling bearings based on enhanced complementary empirical mode decomposition with adaptive noise and statistical time-domain features. Sensors, 19(19), 4047.

[22] Ma, F., Zhan, L., Li, C., Li, Z., & Wang, T. (2019). Self-adaptive fault feature extraction of rolling bearings based on enhancing mode characteristic of complete ensemble empirical mode decomposition with adaptive noise. Symmetry, 11(5), 513.

[23] Wang, L., & Shao, Y. (2020). Fault feature extraction of rotating machinery using a reweighted complete ensemble empirical mode decomposition with adaptive noise and demodulation analysis. Mechanical Systems and Signal Processing, 138, 106545.

[24] Chaabi, L., Lemzadmi, A., Djebala, A., Bouhalais, M. L., & Ouelaa, N. (2020). Fault diagnosis of rolling bearings in non-stationary running conditions using improved CEEMDAN and multivariate denoising based on wavelet and principal component analyses. The International Journal of Advanced Manufacturing Technology, 107(11), 3859-3873.

[25] Yang, L., Hu, Q., & Zhang, S. (n.d.). Research on fault feature extraction method of rolling bearing based on improved wavelet threshold and CEEMD. Journal of Physics: Conference Series, 1449, 012003.

[26] Hou, S., & Guo, W. (2020). Optimal denoising and feature extraction methods using modified EEMD combined with Duffing system and their applications in fault line selection of non-solid-earthed network. Symmetry, 12(4), 536.

[27] Sharma, S., Tiwari, S., & Singh, S. (2019). Diagnosis of gear tooth fault in a bevel gearbox using discrete wavelet transform and autoregressive modeling. Life Cycle Reliability and Safety Engineering, 8(2), 21-32.

[28] Paliwal, D., Choudhury, A., Govardhan, T., & Chandrawat, S. S. (n.d.). A novel approach for detection of bearing defects from noisy vibration signal. Applied Mechanics and Materials, 592, 2001-2005.

[29] Byington, C. S., Orsagh, P. R., Kallappa, P., Sheldon, J., DeChristopher, P., Amin, S., & Hines, J. (2006). Recent case studies in bearing fault detection and prognosis. In 2006 IEEE Aerospace Conference (pp. 1-8). IEEE.

[30] Minnicino, M. A., II, & Sommer, H. J., III. (n.d.). Detecting and quantifying friction nonlinearity using the Hilbert transform. In Health Monitoring and Smart Nondestructive Evaluation of Structural and Biological Systems III (Vol. 5394, pp. 419-427). International Society for Optics and Photonics.

[31] Huang, P., Pan, Z., Qi, X., & Lei, J. (2010). Bearing fault diagnosis based on EMD and PSD. In 2010 8th World Congress on Intelligent Control and Automation (pp. 1300-1304). IEEE.

[32] Huang, N. E., Shen, Z., Long, S. R., Wu, M. C., Shih, H. H., Zheng, Q., Yen, N.-C., Tung, C. C., & Liu, H. H. (1998). The empirical mode decomposition and the Hilbert spectrum for nonlinear and non-stationary time series analysis. Proceedings of the Royal Society of London. Series A: Mathematical, Physical and Engineering Sciences, 454(1971), 903-995.

[33] Wu, Z., & Huang, N. E. (2004). A study of the characteristics of white noise using the empirical mode decomposition method. Proceedings of the Royal Society of London. Series A: Mathematical, Physical and Engineering Sciences, 460(2043), 1597-1611.

[34] Zhen, D., Wang, T., Gu, F., & Ball, A. (2013). Fault diagnosis of motor drives using stator current signal analysis based on dynamic time warping. Mechanical Systems and Signal Processing, 34, 191-202.

[35] Que, Z., & Xu, Z. (2019). A data-driven health prognostics approach for steam turbines based on XGBoost and DTW. IEEE Access, 7, 93131-93138

[36] Pan, Y., Hong, R., Chen, J., Singh, J., & Jia, X. (2019). Performance degradation assessment of a wind turbine gearbox based on multi-sensor data fusion. Mechanism and Machine Theory, 137, 509-526.

[37] Wang, L., Liu, Z., Miao, Q., & Zhang, X. (2018). Complete ensemble local mean decomposition with adaptive noise and its application to fault diagnosis for rolling bearings. Mechanical Systems and Signal Processing, 106, 24-39.

[38] Huo, Z., Zhang, Y., Francq, P., Shu, L., & Huang, J. (2017). Incipient fault diagnosis of roller bearing using optimized wavelet transform based multi-speed vibration signatures. IEEE Access, 5, 19442-19456.

[39] Caesarendra, W., & Tjahjowidodo, T. (2017). A review of feature extraction methods in vibration-based condition monitoring and its application for degradation trend estimation of low-speed slew bearing. Machines, 5(3), 21.

[40] Han, M., & Pan, J. (2015). A fault diagnosis method combined with LMD, sample entropy and energy ratio for roller bearings. Measurement, 76, 7-19.

[41] Singh, A. A., Harikrishnan, C. I., Tiwari, S. K., & Sharma, S. (2023). Investigation on multi-entropy and multi-statistical features fusion approach for fault detection in rolling bearing using VMD. IETE Journal of Research, 69(12), 9245-9250.

[42] Sharma, S., & Tiwari, S. K. (2024). Residual signal-based condition monitoring of planetary gearbox using electrical signature analysis. Journal of Vibration and Control, 30(11-12), 2430-2439.

[43] Sharma, S., & Tiwari, S. K. (2022). A novel feature extraction method based on weighted multi-scale fluctuation based dispersion entropy and its application to the condition monitoring of rotary machines. Mechanical Systems and Signal Processing, 171, 108909.

[44] Sharma, S., Tiwari, S. K., & Singh, S. (2021). Integrated approach based on flexible analytical wavelet transform and permutation entropy for fault detection in rotary machines. Measurement, 169, 108389.

IJEAST

INTERNATIONAL JOURNAL
OF ENGINEERING APPLIED SCIENCE
AND TECHNOLOGY

ABOUT IJEAST

International Journal of Engineering Applied Science and Technology (IJEAST) is a peer-reviewed, open access journal that publishes high-quality research papers in the field of Engineering, Applied Science and Technology.

IJEAST aims to provide a platform for researchers, academicians, and professionals to share their innovative ideas, research findings, and practical experiences with the global scientific community.

FOCUS AREAS

- Engineering
- Applied Science
- Technology
- Innovation & Development
- Interdisciplinary Studies

PEER REVIEWED
All submissions are rigorously peer reviewed to ensure quality.

OPEN ACCESS
Free and unrestricted access to research for all.

GLOBAL REACH
Connecting researchers and professionals worldwide.

TIMELY PUBLICATION
We ensure a swift and efficient publication process.

For more information, visit our website
www.ijeast.com

INTERNATIONAL JOURNAL
OF ENGINEERING APPLIED SCIENCE
AND TECHNOLOGY

editor@ijeast.com
www.ijeast.com
India

2455-2143